Multicolor Electroluminescence from Intermediate Band Solar Cell Structures

*Nair López, Kin Man Yu, Tooru Tanaka, and Wladyslaw Walukiewicz**

Intermediate band solar cells are a new generation of photovoltaics that allow for better utilization of the solar spectrum. The key and most challenging requirement for these cells is an efficient optical coupling between the intermediate band and the charge conducting bands. GaNAs based intermediate band solar cells have been used to generate electroluminescence. Two electroluminescence peaks are generated in the structure with electrically blocked intermediate band. The peaks are observed for both forward and reverse bias configuration and are attributed to optical transitions from the conduction to the intermediate band, and from the intermediate band to the valence band. The origin of the electroluminescence is confirmed by the temperature dependence of the electroluminescence peak energies that is consistent with the band anticrossing model of the intermediate band formation in dilute nitride alloys. This is the first direct observation of the optical transitions required for the operation of intermediate band solar cells. The results also demonstrate that properly modified intermediate band solar cell structures could be used as multicolor light emitters.

1. Introduction

The solar spectrum photons cover a wide range of energies from 0.5 to 4 eV making efficient conversion of the solar light into any other form of energy a challenging task. Thus, there are stringent limits on the maximum power conversion efficiency that can be achieved with a single band gap solar cell.[1] To address this issue and improve the power conversion efficiency a number of approaches have been proposed.[2–10]

Dr. N. López
Departamento de Física Aplicada
Universidad Autónoma de Madrid
C/ Francisco Tomás y Valiente 7
28049 Madrid, Spain
Prof. K. M. Yu
Department of Physics and Materials Science
City University of Hong Kong
Kowloon, Hong Kong
Dr. T. Tanaka
Department of Electrical and Electronic Engineering
Saga University
Saga 840-8502, Japan
Prof. W. Walukiewicz
Materials Sciences Division
Lawrence Berkeley National Laboratory
1 Cyclotron Road, Berkeley, CA 94720, USA
E-mail: w_walukiewicz@lbl.gov

DOI: 10.1002/aenm.201501820

The concept of multiband or intermediate solar cell (IBSC) has been proposed more than 50 years ago.[2] There have been numerous attempts to find a material system that could satisfy the stringent requirements for the cell operation. The current status of the field has been recently reviewed by Okada et al.[11] The first fully operational IBSC has been practically realized using GaNAs, a dilute nitride alloy belonging to the class of highly mismatched alloys (HMAs).[12] The energy band structure of HMAs is determined by the interaction between localized states of the minority component (N) and extended conduction band states of the matrix (GaAs). This initial progress was further advanced in studies of IBSCs with GaInNAsSb[13,14] and ZnOTe[15] HMA absorbers.

A critical issue for the HMA based IBSCs is the strength of three optical transitions coupling the valence, intermediate and the conduction band. Although the contribution of a sequential absorption of two photons on the IBSC photocurrent has been recently observed[13,15] there has been no direct observation of the optical transitions between the intermediate and upper conduction band. Here we demonstrate that a unique distribution of the electric field in an IBSC allows observation of the two reverse-bias electroluminescence bands originating from the transitions between the intermediate and the conduction and the valence bands. The origin of these optical transitions is confirmed by the temperature dependence of the emitted photon energies deduced from the band anticrossing (BAC) model of the electronic band structure of GaNAs.[16–21]

2. Experimental Results

The IBSC device structures shown in **Figure 1** were grown using metalorganic chemical vapor deposition (MOCVD).[22] Two types of structures were grown. In the BIB structure shown in Figure 1a the intermediate band is electrically isolated from the contacts, whereas in the unblocked intermediate band (UIB) structure, shown in Figure 1b the intermediate band is connected to the back side contact. As has been shown previously,[12] the BIB structure operates as an IBSC, whereas the UIB structure works as a PV device with the energy band gap given by energy difference between intermediate and the valence band. Two BIB structures have been grown

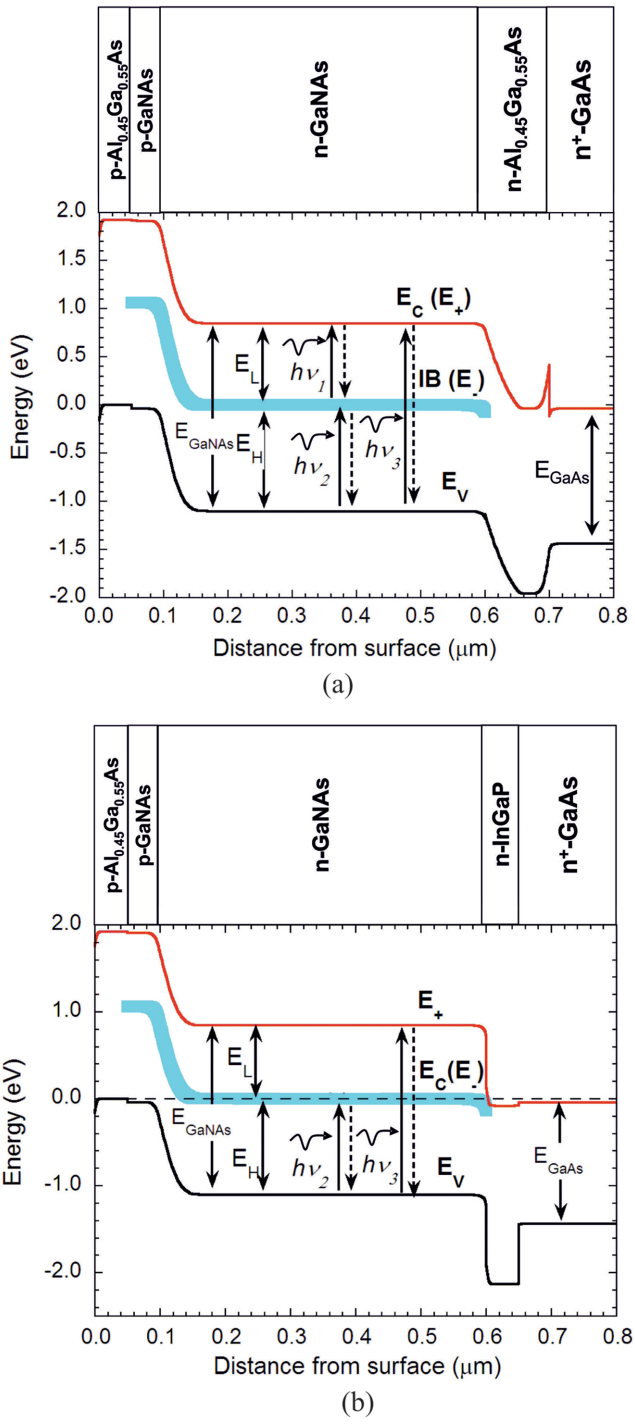

Figure 1. a) Blocked intermediate band (BIB) structure with the intermediate band isolated from contacts and two, front and back side, depletion regions. b) A reference unblocked intermediate band (UIB) solar cell structure with the intermediate band electrically connected to the back contact and a single, front side, depletion region.

with different N concentrations. Structures with 3.1% and 3.8% N content are labeled as devices "1" and "2," respectivey.

The photovoltaic performance of the structures has been studied before.[12,23] Typical current–voltage characteristics

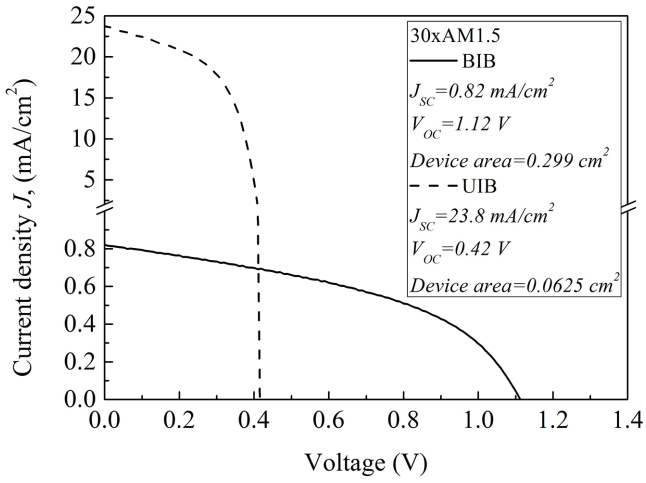

Figure 2. Current voltage characteristics for blocked (solid black line) and unblocked (dashed black line) intermediate band solar cell structures.

obtained in UIB and BIB structures are shown in **Figure 2**. The results represent the first experimental evidence for the quasi-Fermi level splitting and first operational intermediate band solar cell.[12,23] The electroluminescence (EL) measurements were performed in the temperature range from 20 to 300 K. An alternating electrical current was applied to the devices placed in a liquid He cryostat. The emitted light passing through a monochromator was detected by a Ge detector using a lock-in amplifier.

Electroluminescence spectra of both UIB and BIB structures under forward bias are shown in **Figure 3**. The UIB structure shows a single peak, at about 1.15 eV corresponding to the transition from the IB (E_-) to the valence band (E_V) (E_H in Figure 1). This is consistent with the energy band diagram shown in Figure 1b where only one depletion region in the top part of the device is present. A forward bias produces occupation inversion resulting in the optical transition between the E_- and the E_V.

A more complex EL spectrum is observed in the BIB structure. It consists of two broad low energy peaks E_L and E_H and a higher energy emission (E_3) with a maximum at about 1.35 eV. This high energy emission cannot originate from any transitions within the absorber layer. We have tentatively attributed this high energy emission to transitions involving heavily doped substrate and the AlGaAs blocking layer in the back-side depletion region.

As seen in Figure 3 the electroluminescence peak denoted E_H coincides with the emission peak found in UIB structure and can be attributed to the transitions from E_- to E_V, whereas the weak, low energy emission denoted as E_L appears to be close to the energy separation between the E_+ and E_- bands. This is a significant result as it appears to be the first direct observation of optical transitions between those two bands. The observation of these two transitions is the reflection of the fact that there are two depletion regions in the BIB device; one in the front part (close to the surface) and the other one in the back of the structure (close to the GaAs substrate). The applied voltage is distributed among those two regions. This is illustrated in the schematic band diagram of the BIB structure under forward bias shown in **Figure 4**a. At the back side depletion region

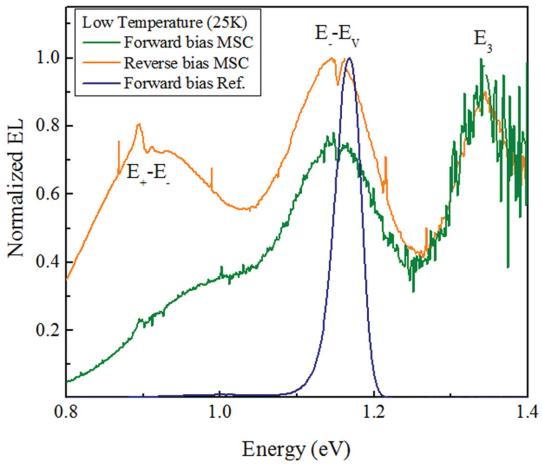

Figure 3. Low temperature electroluminescence in blocked and unblocked intermediate band solar cell structures for forward and reverse bias conditions. Green line and orange line correspond to forward and reverse bias electroluminescence from BIB structure, respectively. Blue line represents forward bias electroluminescence from the UIB structure.

electrons that are injected from the substrate to the upper conduction band E_+ recombine radiatively with holes in the partially occupied intermediate band, giving rise to a low energy emission (E_L). On the other hand, the higher energy emission (E_H) originates from the front side depletion region where electrons injected to the p-type region of the IB recombine with the holes in the valence band.

To further investigate these transitions we have measured the EL spectra under reverse bias conditions. No reverse-bias EL was found in the UIB structure confirming that the structure is equivalent to a single p-n junction. However, as seen in Figure 3, a well resolved two band EL spectrum is found in the BIB structure. Most notably a very strong low energy emission, E_L, with the peak energy at about 0.9 eV is clearly observed under the reverse bias conditions.

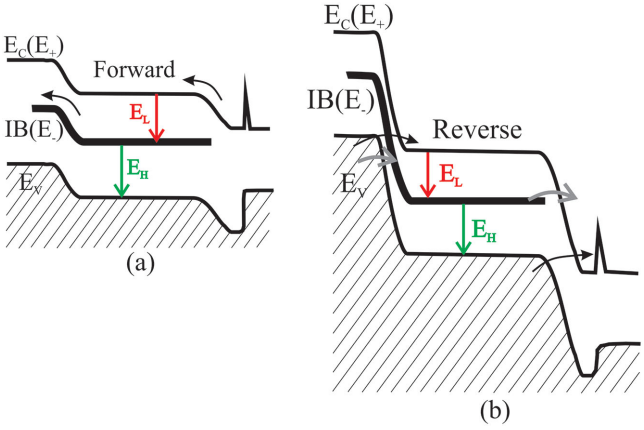

Figure 4. Schematic illustration of the electroluminescence emission mechanism in the BIB structure under a) forward and b) reverse bias conditions.

3. Discussion

These unusual results can be understood only assuming that the partially occupied intermediate band (IB) (E_-) band is electrically isolated from the contacts in the blocked intermediate band (BIB) structure. When a reverse bias is applied to the BIB structure the total potential drop is distributed between the front side and the back side depletion regions. The mechanism of the two photon EL generation is schematically shown in Figure 4b. At the front side depletion region a high enough reverse bias voltage shifts the valence band up and injects electrons from the valence band to the intermediate band and the conduction band, E_C (E_+). At the back side depletion region the reverse bias shifts down the conduction band of the GaAs substrate and injects holes into the intermediate band and the valence band. As a result an occupation inversion, with electrons in the E_+, holes in the E_V and electrons and holes in the IB are established in the middle of the BIB structure. This results in emission associated with optical transitions between E_C and IB (E_L) as well as between IB and E_V (E_H).

Although both E_L and E_H emissions are observed for the forward and reverse bias conditions, there is an important difference in the relative intensity of those two emissions under different bias conditions. Thus, as seen in Figure 3, the E_L emission is much stronger under reverse bias. This is consistent with the schematic picture illustrating the origin of the E_L and E_H shown in Figure 4. Under forward bias the strong E_H emission originates from the front part of the structure, whereas a weak E_L emission is mostly generated on the back side. By contrast, under reverse bias the much stronger E_L emission is generated in the front side depletion region.

In principle, as evident from Figure 4b, for the reverse bias it should be possible to observe an even higher energy emission originating from radiative recombination of electrons injected to the E_C at the front side and holes injected to the E_V in the back side depletion region. However, this is unlikely in the studied devices as it would require long electron and/or hole diffusion lengths to diffuse across the 0.5 μm thick absorber layer. However, a modified structure with thinner mid-part absorber layer could possibly be used to observe all three optical transitions.

A possible concern is that the E_L emission may be defect related, i.e., originate from optical transitions between localized defect states and the E_V, or E_- band. To address this concern we have measured temperature dependence of the emission bands. **Figure 5** shows evolution of the emission band energies as functions of temperature in both BIB structures. Although the two separate peaks could be resolved only for temperatures lower than ≈150 K, it is clearly seen that the E_L emission band shifts to higher and the E_H emission band to lower energy with increasing temperature.

The energies of the E_L and E_H emission maxima were determined by fitting the spectra in Figure 5 with Gaussian curves. The results are shown **Figure 6**. In both devices the temperature coefficients for the E_L peak are positive and equal to $+2.9 \times 10^{-4}$ eV K^{-1} for device 1 and $+1.7 \times 10^{-4}$ eV K^{-1} for device 2, whereas the temperature coefficient for the maximum energy of the E_H peak are negative and equal to -1.1×10^{-4} eV K^{-1} for device 1 and -1.5×10^{-4} eV K^{-1} for device 2.

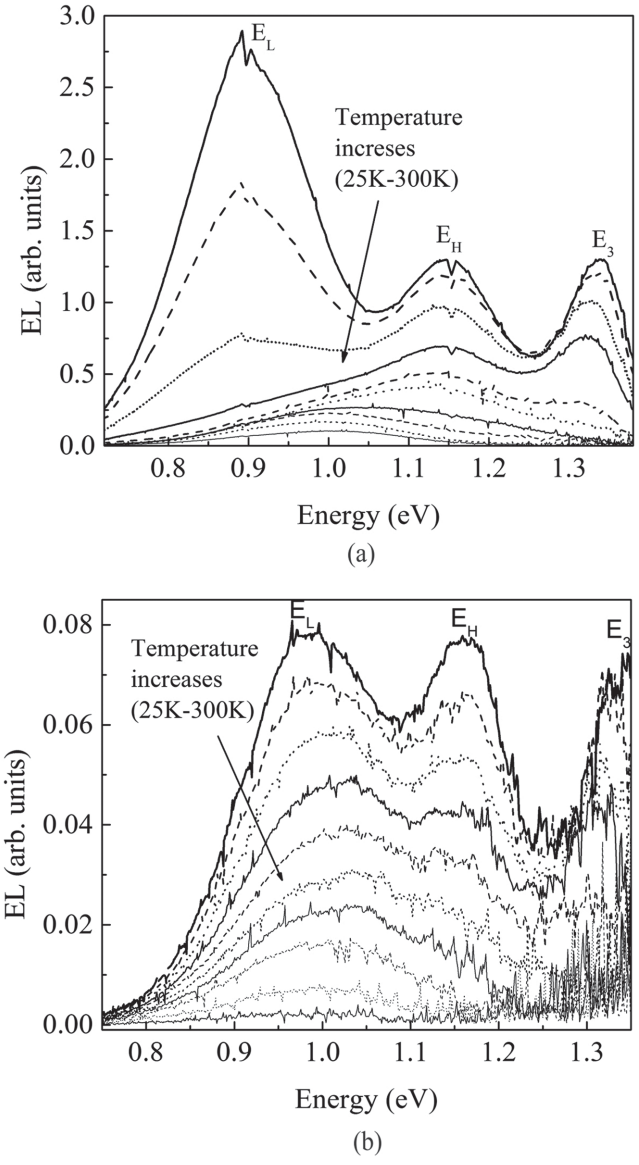

Figure 5. Temperature dependence of the electroluminescence spectra a) for the BIB device 1 and b) for the BIB device 2. Different lines denote spectra measured at different temperatures.

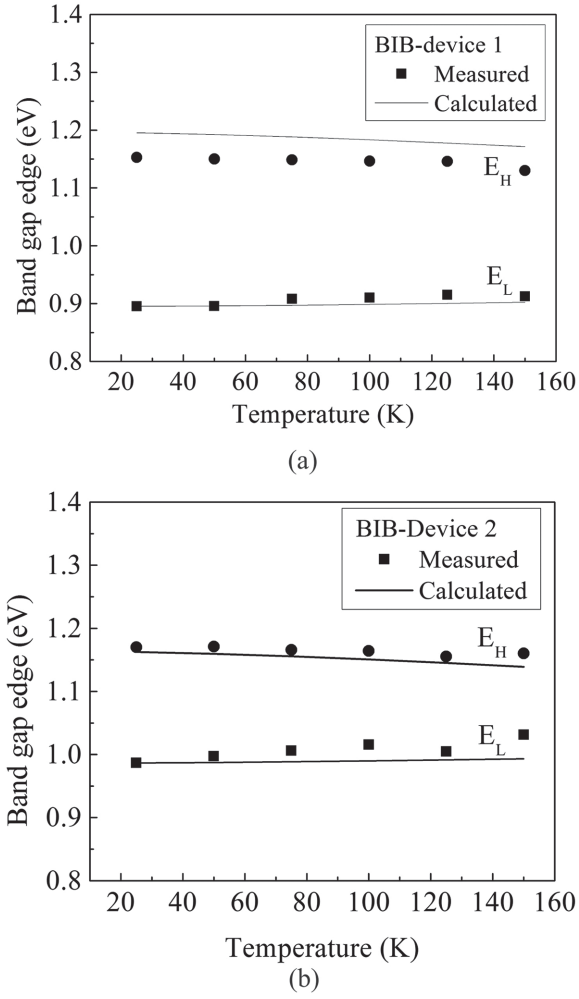

Figure 6. The temperature dependence of the electroluminescence energy peaks (E_H and E_L). Solid circles and squares represent experimental values for E_H and E_L, respectively. The lines represent a theoretical fit using BAC model a) for BIB device 1 and b) for BIB device 2.

The unusual positive temperature coefficient for the E_L emission peak can be well understood assuming that the emission originates from the transition between E_+ and E_- bands.

The energies of the E_+ and E_- sub-band edges are given by the BAC model[16,17] in Equation (1)

$$E_{\pm} = \frac{\left(E_N + E_M(T)\right) \pm \left[\left(E_N - E_M(T)\right)^2 + 4C_{NM}^2 x\right]^{1/2}}{2} \quad (1)$$

where E_N is the energy of the localized nitrogen level, E_M is the conduction band edge of the GaAs matrix and C_{NM} = 2.7 eV is the coupling constant.[16] With the vacuum level as reference energy it can be assumed that the energy of the highly localized N level does not depend on temperature. Therefore the temperature dependence for the E_+ to E_- transitions is given by (Equation (2)

$$\frac{d(E_+ - E_-)}{dT} = \frac{\left(E_M(T) - E_N\right)\frac{dE_M(T)}{dT}}{\sqrt{\left(E_N - E_M\right)^2 + 4C_{NM}^2 x}} \quad (2)$$

The temperature coefficient is positive as the terms dE_M/dT and $(E_M - E_N)$ are negative. This accounts for the observed increase of the E_L emission peak energy with increasing temperature. Such uncommon temperature behavior can be attributed to the fact that for E_N located above E_M the $E_+ - E_-$ energy difference is controlled by the BAC interaction rather than the shift of E_M. The positive temperature coefficient excludes a possibility that the E_L peak could originate from transitions between a deep level and either the E_- or the E_V bands, since in both cases the transition energy is expected to decrease with increasing temperature because of the upward shift of the E_V and the downward shift of the E_- on the absolute scale. Also, the

negative temperature coefficient for the E_H peak is consistent with transitions between E_- and the valence band edge.

The observed two color EL is an unusual feature specific to the BIB structure. This demonstrates that such structures could be used as multicolor emitters. Also, in addition to the two observed emission bands a larger energy emission originating from recombination of the electrons injected into the E_C (E_+) at the front junction and holes injected into the E_V at the back junction should be also possible. This, however, would require a thinner absorber layer that separates the front and back junction.

4. Conclusions

We have provided the first experimental evidence for direct optical coupling between the intermediate band and the charge conducting bands in an intermediate band solar cell structure. Two electroluminescence emission peaks are observed under reverse and forward bias due to the presence of a front and a back depletion region in the BIB structure. The emission bands show characteristic temperature dependence that confirms the role of band anticrossing in the formation of the intermediate band in dilute GaNAs. The results demonstrate that properly modified IBSC-like structures could be used as multicolor light emitters.

Acknowledgements

This work was performed at the EMAT, LBNL and was supported by the Director, Office of Science, Office of Basic Energy Sciences, Materials Sciences and Engineering Division, of the U.S. Department of Energy under Contract No. DE-AC02-05CH11231. N.L. acknowledges support from the European Commission by Marie Curie International Incoming Fellowship PIIF-GA-2012-326579 and from LBNL's LDRD fund. W.W. and K.M.Y. designed the IBSC structures and provided the interpretation of the experimental results. N.L. fabricated the devices and performed the electroluminescence measurements. All the authors discussed the results and N.L. and W.W. wrote the manuscript. Material growth and device fabrication was partially supported by RoseStreet Labs Energy.

Received: September 11, 2015
Revised: October 27, 2015
Published online: December 12, 2015

[1] W. Shockley, H. J. Queisser, *J. Appl. Phys.* **1961**, *32*, 510.
[2] M. Wolf, *Proc. IEEE IRE.* **1960**, *48*, 1246.
[3] A. M. Green, *Prog. Photovolt.: Res. Appl.* **2001**, *9*, 137.
[4] W. Guter, J. Schöne1, S. P. Philipps, M. Steiner, G. Siefer, A. Wekkeli, E. Welser, E. Oliva1, A. W. Bett, F. Dimroth, *Appl. Phys. Lett.* **2009**, *94*, 223504.
[5] A. M. Green, *Mater. Sci. Eng. B* **2000**, *74*, 118.
[6] T. Trupke, P. Würfel, M. A. Green, presented at *3rd World Conf. Photovoltaic Energy Conversion*, Osaka, Japan, May 2003.
[7] N. S. Lewis, *Science* **2007**, *315*, 798.
[8] M. Law, L. E. Greene, J. C. Johnson, R. Saykally, P. Yang, *Nat. Mater.* **2005**, *4*, 455.
[9] R. J. Chaffin, G. C. Osbourn, L. R. Dawson, R. M. Biefeld, in *Conf. Record 17th IEEE Photovoltaic Specialists Conf.*, Kissimmee, Florida, USA **1984**, pp. 743.
[10] A. Luque, A. Martí, *Phys. Rev. Lett.* **1997**, *78*, 5014.
[11] Y. Okada, N. J. Ekins-Daukes, T. Kita, R. Tamaki, M. Yoshida, A. Pusch, O. Hess, C. C. Phillips, D. J. Farrell, K. Yoshida, N. Ahsan, Y. Shoji, T. Sogabe, J.-F. Guillemoles, *Appl. Phys. Rev.* **2015**, *2*, 021302.
[12] N. López, L. A. Reichertz, K. M. Yu, K. Campman, W. Walukiewicz, *Phys. Rev. Lett.* **2011**, *106*, 028701.
[13] N. Ahsan, N. Miyashita1, M. M. Islam, K. M. Yu, W. Walukiewicz, Y. Okada, *Appl. Phys. Lett.* **2012**, *100*, 172111.
[14] R. Tamaki, Y. Shoji, Y. Okada, K. Miyano, *Appl. Phys. Lett.* **2014**, *105*, 073118.
[15] T. Tanaka, M. Miyabara, Y. Nagao, K. Saito, Q. Guo, M. Nishio, K. M. Yu, W. Walukiewicz, *Appl. Phys. Lett.* **2013**, *102*, 052111.
[16] W. Shan, W. Walukiewicz, J. W. AgerIII, E. E. Haller, J. F. Geisz, D. J. Friedman, J. M. Olson, S. R. Kurtz, *Phys. Rev. Lett.* **1999**, *82*, 1221.
[17] W. Walukiewicz, W. Shan, K. M. Yu, J. W. AgerIII, E. E. Haller, I. Miotlowski, M. J. Seong, H. Alawadhi, A. K. Ramdas, *Phys. Rev. Lett.* **2000**, *85*, 1552.
[18] W. Shan, W. Walukiewicz, K. M. Yu, J. W. AgerIII, E. E. Haller, J. F. Geisz, D. J. Friedman, J. M. Olson, S. R. Kurtz, C. Nauka, *Phys. Rev. B* **2000**, *62*, 4211.
[19] K. M. Yu, W. Walukiewicz, J. Wu, W. Shan, J. W. Beeman, M. A. Scarpulla, O. D. Dubon, P. Becla, *Phys. Rev. Lett.* **2003**, *91*, 246403.
[20] J. F. Geisz, D. J. Friedman, *Semicond. Sci. Technol.* **2002**, *17*, 769.
[21] K. M. Yu, W. Walukiewicz, J. W. AgerIII, D. Bour, R. Farshchi, O. D. Dubon, S. X. Li, I. D. Sharp, E. E. Haller, *Appl. Phys. Lett.* **2006**, *88*, 092110.
[22] F. Dimroth, C. Baur, A. W. Bett, K. Volz, W. Stolz, *J. Cryst. Grow.* **2004**, *272*, 726.
[23] N. López, L. A. Reichertz, K. M. Yu, K. Campman, W. Walukiewicz, in *Proc. 26th Eur. Int. Conf. Photovoltaic Solar Energy*, WIP – Renewable Energies, pp. 97–100, Munich **2011**.

